Energy and Buildings, 17 (1991) 43–54

Influence of air infiltration on airflow in a ventilated isothermal two-zone enclosure

J. C. Y. Wang, Z. Jiang and F. Haghighat

Centre for Building Studies, Concordia University, Montreal, Que., H3G 1M8 (Canada)

(Received February 10, 1990; accepted March 15, 1990; revised paper received June 25, 1990)

Abstract

Influences of air infiltration on the airflow and contaminant distribution in a ventilated isothermal two-zone enclosure are investigated by numerical simulation. The direction of infiltration airflow is considered to be in the opposite direction of the room ventilation air. The enclosure is divided into two zones, zone A and zone B, by a partition with a door opening. The ventilation air flows into zone A (namely ventilation zone) through a rectangular supply opening near the floor on the end-wall of the zone and leaves the enclosure through a ceiling-mounted exhaust opening in zone B. The infiltration air flows uniformly into zone B (namely infiltration zone) through the other end-wall, and leaves through the exhaust. Three different values of air infiltration rate are considered. In the analysis of the combined influence of door-opening position and infiltration on the air movement, the door opening is placed at three positions, namely, $y_D/W = 0.167$, 0.5 and 0.833 respectively. The airflow is considered to be three-dimensional and fully turbulent. The predicted results indicate that a local exhaust will effectively limit the transportation of the contaminant from the infiltration zone into the ventilation zone, and the effect of infiltration on its downstream zone could be negligibly small, if the door opening and the exhaust are properly placed.

1. Introduction

Detailed knowledge of airflow, contaminant dispersion and fire-induced smoke migration in buildings is required in design and control of ventilation systems and development of control strategies. So far, the design of ventilation systems has been based on the air speed model [1], rather than the air velocity model. In other words, the whole air velocity field in a zone is taken as uniform. Recent investigation has shown that the variation of air velocity and contaminant concentration in each zone of a multi-zone building sometimes could not be neglected [2, 3]. For instance, the air velocities, temperature variations and contaminant concentration might be under the acceptable level at certain places, but in excess at other areas. The difference in their magnitude from point to point could be remarkably large. Consequently, better understanding of air velocity, temperature, and contaminant concentration distributions in enclosures has attracted more and more attention.

The airflow pattern in a single ventilated enclosure has been investigated by many researchers [2, 4–7]. For a single ventilated enclosure, the airflow pattern is affected by the supply and return arrangements, the size and the shape of enclosures, the velocity at the supply opening, the air infiltration or exfiltration and so on. When ventilation is combined with heating or cooling function, the buoyancy force will also be a factor influencing the air movement in the enclosure.

For enclosures separated by a partition with an opening on it, the opening size and position are additional factors affecting the airflow patterns. Chang *et al.* [8], Kelkar and Patankar [9], and Haghighat *et al.* [10] numerically conducted their investigations on the effect of partition, while Nansteel and Greif [11], Scott

0378-7788/91/$3.50

et al. [12], Epstein [13], Neymark *et al.* [14], and Boardman *et al.* [15] experimentally studied the same subject. These works concerned mainly the inter-zone natural convection. In a ventilated two-zone enclosure, especially when the ventilation supply and exhaust openings are located in different zones, the effect of the door-opening position on air movement may be different from that in the natural convection case. Haghighat *et al.* [16] studied the airflow patterns in a partitioned enclosure for one case with a ventilation boundary condition and the other with an infiltration boundary condition. That is, when the air movement caused by ventilation was studied, no air infiltration was considered, and inversely, in the infiltration study, the ventilation was not taken into consideration. In practice, however, the air infiltration may take place at an exterior wall of a ventilated room, and may make a significant difference on the air movement and the contaminant distribution in a ventilated two-zone enclosure. For instance, when a ventilated living area is separated from a kitchen by a partition, infiltration in the kitchen may bring some unexpected contaminants into the living area.

The present study is a continuation of the investigation carried out by Haghighat *et al.* [16]. The purpose of the present study is:

(1) to examine the effect of the air infiltration on the airflow pattern and contaminant distribution in a ventilated isothermal two-zone enclosure;

(2) to investigate how the ventilation zone zone A, is affected by the source in the infiltration zone, zone B, under various door positions.

The approach adopted is numerical simulations. For the sake of simplification, the air infiltration in this study is assumed to be uniformly distributed over the entire exterior wall. Different infiltration flow rates are considered to represent different outdoor conditions, while the ventilation airflow rate is kept at a constant value in all cases. The degree of air infiltration affecting contaminant distribution in the ventilated two-zone enclosure will also be described.

2. Problem statement

A two-zone enclosure with dimensions of $L=10$ m, $H=3$ m, and $W=4$ m is shown in Fig. 1. A partition is inserted at the middle of the enclosure dividing the enclosure into two equal-sized zones, zone A and zone B. The two zones are connected through a door opening in the partition. The ventilation supply and exhaust are located on the end-wall of zone A and the ceiling of zone B respectively. A contaminant source with a unit emission rate is placed right under the exhaust opening near

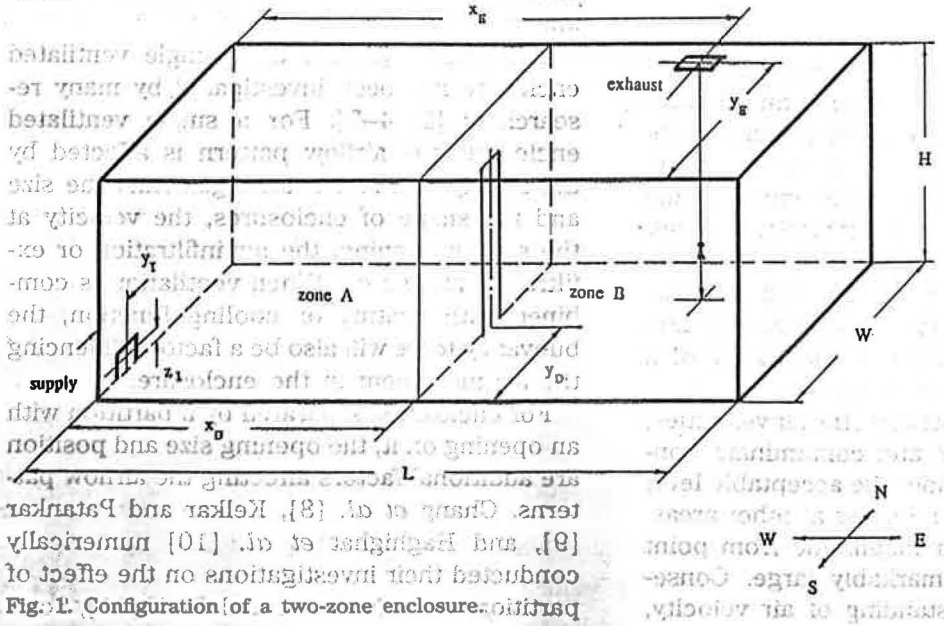

Fig. 1. Configuration of a two-zone enclosure.

the floor. Wall E, the end-wall in zone B, is considered to be an exterior wall. A uniform air infiltration takes place through this wall into the enclosure. The sizes and positions of the door, supply and exhaust are listed in Table 1.

When there is no air infiltration from wall E into the enclosure, zone A is free from the contaminant, because the contaminant source is in zone B, the downstream zone of the ventilating airflow. However, when air infiltration takes place at wall E, the contaminant may be blown into zone A by the infiltrating air, if the infiltration airflow is large enough in comparison with ventilation airflow. In this case, the air velocities at the door opening are not all in the direction from zone A to zone B anymore, and a counterflow will appear at the door opening. It could be expected that, for various door positions, the effect of infiltration airflow on velocity distribution at the door opening is different.

In order to reveal these phenomena, three infiltration flow rates 1.8 ach, 3.6 ach, and 10.8 ach, equivalent to air velocities, 0.005 m/s, 0.01 m/s and 0.03 m/s are simulated. The door opening size remains unchanged, while the door opening position is varied by moving it along the partition in the y direction to three different positions $y_D/W=0.167$, 0.5 and 0.833 respectively. The ventilation air velocity at the supply opening has the value of 1.0 m/s for all cases in this study.

3. Physical foundation

The Reynolds number, Re, in the present study is more than 1.6×10^4 when the velocity at the ventilation supply is 1.0 m/s (2.5 ach). In this case, the flow is expected to be turbulent

TABLE 1. The dimension and location of the opening

	Donor	Supply	Exhaust	Source
Dimension				
b/W	0.17	0.083	0.083	–
h/H	0.75	0.083	–	–
l/L	–	–	0.056	–
Location				
x/L	0.5	0.0	0.75	0.75
y/W	Variable	0.125	0.875	0.875
z/H	–	0.042	1.0	0.125

[17]. Consequently, the high-Reynolds-number k–ϵ two-equation model of turbulence [18] is adopted. The two variables k and ϵ represent the kinetic energy of turbulence and the dissipation rate of turbulent energy respectively. They are obtained from their own conservation equations.

For three-dimensional incompressible, isothermal turbulent flow, the variables to be solved are the velocity components in the x, y and z directions, the contaminant concentration, c, the kinetic energy of turbulence, k, and the dissipation rate of turbulent energy, ϵ. The governing equations can be written in the following general form.

$$\frac{\partial(\rho\phi)}{\partial t}+\frac{\partial(u_i\rho\phi)}{\partial x_i}=\frac{\partial}{\partial x_i}\left(\Gamma_{\phi,\,\mathrm{eff}}\frac{\partial\phi}{\partial x_i}\right)+S_\phi \qquad (1)$$

where ϕ denotes variables, and S_ϕ represents the source term for the corresponding variable, and is listed in Table 2. $\Gamma_{\phi,\,\mathrm{eff}}$ is the effective exchange coefficient which may be calculated as follows,

$$\Gamma_{\mathrm{eff}}=\frac{\mu_{\mathrm{eff}}}{\sigma_\phi}=\frac{\mu}{\sigma}+\frac{\mu_t}{\sigma_t} \qquad (2)$$

where σ stands for Prandtl or Schmidt number; μ_t is the turbulent viscosity which may be determined by k and ϵ as

$$\mu_t=C_\mu\rho k^2/\epsilon \qquad (3)$$

In order to simplify the problem, the following assumptions are made:

(1) the thickness of the partition is small relative to the length of the enclosure and may be neglected;

(2) the contaminant source is considered to be a point source, namely, it does not have any physical volume;

(3) one-phase flow assumption is employed, in other words, there is no relative velocity between the contaminant particles and the air.

4. Numerical procedure

The numerical computation is performed on $20\times14\times14$ uniform control volumes. The discretization of the governing differential equation, eqn. (1), into finite-difference form is fulfilled by integrating the governing equation over each control volume. Based on a staggered mesh system, the Hybrid Scheme is used to

TABLE 2. Source term for conservation equation

ϕ	Γ_ϕ	S_ϕ
1	0	0
u	μ_{eff}	$-\frac{\partial p}{\partial x}+\frac{\partial}{\partial x}\left(\mu_{eff}\frac{\partial u}{\partial x}\right)+\frac{\partial}{\partial y}\left(\mu_{eff}\frac{\partial v}{\partial x}\right)+\frac{\partial}{\partial z}\left(\mu_{eff}\frac{\partial w}{\partial x}\right)$
v	μ_{eff}	$-\frac{\partial p}{\partial y}+\frac{\partial}{\partial x}\left(\mu_{eff}\frac{\partial u}{\partial y}\right)+\frac{\partial}{\partial y}\left(\mu_{eff}\frac{\partial v}{\partial y}\right)+\frac{\partial}{\partial z}\left(\mu_{eff}\frac{\partial w}{\partial y}\right)$
w	μ_{eff}	$-\frac{\partial p}{\partial z}+\frac{\partial}{\partial x}\left(\mu_{eff}\frac{\partial u}{\partial z}\right)+\frac{\partial}{\partial y}\left(\mu_{eff}\frac{\partial v}{\partial z}\right)+\frac{\partial}{\partial z}\left(\mu_{eff}\frac{\partial w}{\partial z}\right)$
k	$\frac{\mu_{eff}}{\sigma_k}$	$G_k-\rho\epsilon$
ϵ	$\frac{\mu_{eff}}{\sigma_\epsilon}$	$C_1\frac{\epsilon}{k}G_k-C_2\frac{\rho\epsilon^2}{k}$
c	$\frac{\mu_{eff}}{\sigma_c}$	0

cast difference equations for velocity components, k and ϵ, while the upwind scheme is adopted for contaminant concentration. The coupled difference equations are solved through SIMPLE procedure [19]. A modification is made by adding an overall continuity correction in the x direction. The overall velocity correction ensures the same amount of air flowing through each section parallel to the partition in each iteration. It can be expressed as

$$\sum_i (u_i+\Delta u)A_i = Q_{up} \tag{4}$$

where Δu is the overall velocity correction term, a constant for each control volume in the same section. The summation is carried out over the whole section perpendicular to the x direction.

From eqn. (4), the overall velocity correction can be calculated. It is

$$\Delta u = \frac{Q_{up}-Q}{\sum_i A_i} \tag{5}$$

where Q represents the volume airflow rate across the section being computed before velocity is corrected overall.

The iteration procedure is carried out by the ADI method with the false time-step. The turbulent wall functions [20] are applied to describe the properties at the grids near the solid surfaces. However, there is an exception for wall E from where air infiltrates, owing to the boundary layer near this wall being destroyed by the penetrating air. The air velocities at the supply and exhaust openings are considered to be uniformly distributed over the entire area of the openings.

5. Results

5.1. Effect of the air infiltration on the airflow and contaminant distributions in a ventilated two-zone enclosure

The direction of infiltration airflow is considered to be in the opposite direction to the air velocity at the ventilation supply. The air uniformly infiltrates through wall E with velocity U_{INF}. In order to examine the effect of this infiltration on general patterns of airflow, three different air infiltration velocities, $U_{INF}=0.005$ m/s (1.8 ach), 0.01 m/s (3.6 ach) and 0.03 m/s (10.8 ach), were considered, while the ventilation air velocity was kept at $U_I=1.0$ m/s (2.5 ach), and the door position was fixed at $y_D/W=0.167$.

Figure 2 illustrates the airflow pattern at the vertical section $y/W=0.46$ where the airflow is blocked by the partition. The flow patterns in zone A do not seem to be quite different although the air infiltration flow rate at wall E in zone B is increased considerably from Fig. 2(a) through Fig. 2(c). In zone B, the increment of air infiltration results in increasing areas with a one-dimensional tendency. This is attributed to the uniform and one-dimen-

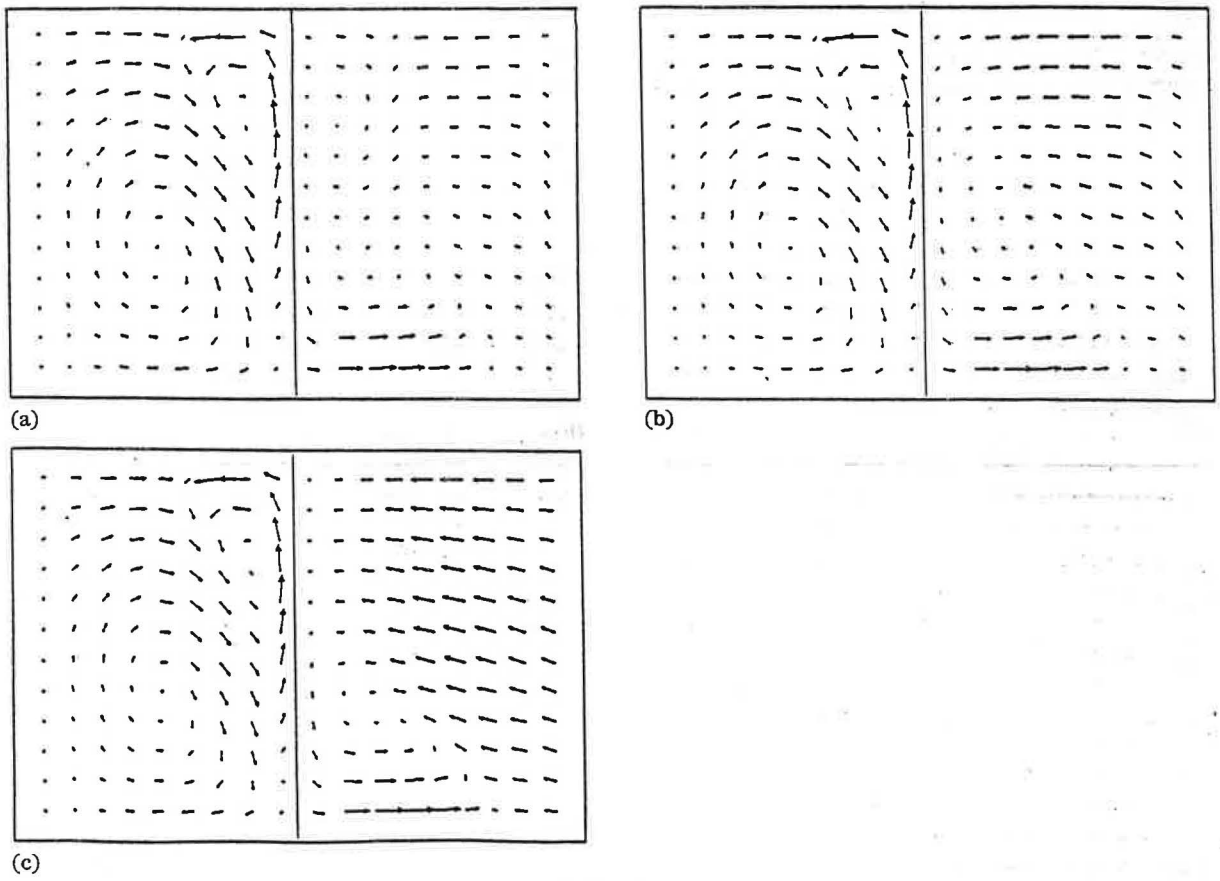

(a) (b) (c)

Fig. 2. Velocity vectors in vertical section, $y/W=0.46$, for the case with $y_D/W=0.167$. (a) $U_{INF}=0.005$, maximum vector, $0.770E-1$. (b) $U_{INF}=0.01$, maximum vector, $0.753E-1$. (c) $U_{INF}=0.03$, maximum vector $0.782E-1$.

sional infiltration assumption. When U_{INF} increases to 0.03 m/s, infiltration airflow dominates in zone B, and the air vortex area is significantly restricted by infiltration airflow (Fig. 2(c)).

The velocity vectors in horizontal sections, $z/H=0.29$ and $z/H=0.79$ are shown in Fig. 3. The airflow pattern and the strength of the air circulation in zone A are similar again for the two different infiltration rates just as those in the vertical section $y/W=0.46$. In other words, the infiltration exerts little influence on the airflow in this zone. In zone B, the effect of the infiltration is not apparent at the lower section of $z/H=0.29$. This is due to the fact that the supply is at a lower position, and the momentum of the ventilation flow at the lower section is larger than that of infiltration, despite that the total flow rate by infiltration is close to that by ventilation. When the horizontal plane rises to $z/H=0.79$ (Figs. 3(c) and 3(d)), the influence of the ventilation flow becomes smaller than that at section $z/H=0.29$, while the momentum of the infiltration flow keeps the same as that at the lower section. The air movement for the case with $U_{INF}=0.03$ is seen to be completely dominated by air infiltration as shown in Fig. 3(d).

Corresponding to the airflow in Fig. 3, Fig. 4 presents the distribution of contaminant concentration in horizontal sections, $z/H=0.29$ and 0.79 respectively. As mentioned earlier, at the section $z/H=0.29$, where the infiltration momentum is relatively small, the contaminant dispersion at the section is mainly controlled by ventilation airflow, therefore the increment of infiltration does not cause a big difference in the concentration distribution as shown in Figs. 4(a) and 4(b). At the higher level $z/H=0.79$, where the infiltration prevails over ventilation flow, the average concentration with $U_{INF}=0.01$ is higher than that with $U_{INF}=0.03$ in both zones.

Distributions of the air velocity component in the x direction at the axis of the door opening for three infiltration velocities are shown in Fig. 5(a). The supply is located near the floor, therefore, air velocities at the lower part of the door opening are relatively strong, and the infiltration airflow cannot compete with it. At the upper part of the door opening where the airflow caused by ventilation is relatively weak, the resultant velocity in the x direction has a negative value. This indicates that the airflow induced by infiltration has a chance to enter zone A. When the infiltration flow rate increases, the negative velocity at the upper part of the door opening becomes larger. To ensure mass balance, the positive velocity at the lower part of the opening must increase.

The average contaminant concentrations in each zone with different air infiltration rates from wall E are presented in Table 3. It indicates that the increment of the air infiltration lowers the average concentration in both zones.

5.2. Effect of the door position on the airflow and contaminant distribution in a ventilated two-zone enclosure

To investigate the effects of door position on the airflow pattern, three different positions, $y_D/W=0.167$, 0.5 and 0.833 are examined respectively, while the ventilation and infiltration rate remain unchanged. The velocity of the room ventilation air at supply opening remains 1.0 m/s. The infiltration air velocity is taken as 0.03 m/s to model an extremely strong infiltration.

The airflow patterns at the vertical section, $y/W=0.46$, for three different door positions are illustrated in Fig. 6. In zone A the infiltration action can hardly be seen, and the flow pattern is not sensitive to the position of the door opening. However, the velocity level is lower when the door opening is at $y_D/W=0.167$, and the action of ventilation airflow in the lower area of zone B is stronger than the other two cases, because the ventilation air can enter zone B more easily in this case than in the other two cases. Figures 7 and 8 demonstrate the flow patterns at the horizontal section, $z/H=0.29$ and 0.79 respectively. In Figs. 7(b) and 7(c), since the air circulation in zone B is relatively weak, the infiltration airflow seems to dominate the flow field, and the flow patterns are similar. In Fig. 7(a), the infiltration effect is less strong for the reason presented earlier.

At the section $z/H=0.79$, where zone A and zone B are completely separated by the door soffit, no effect of door position on flow pattern can be seen in both zone A and zone B. The ventilation flow is dominant in zone A, while in zone B, the infiltration flow is more pronounced as shown in Fig. 8.

The contaminant concentrations corresponding to Fig. 7 are illustrated in Fig. 9. Once again, it is observed that the concentration distributions in Fig. 9(b) and 9(c) are in a similar form, and zone A is almost free from being contaminated in these two cases. In Fig. 9(a), the highest concentration seems to be lower than that in the other two cases. However, the concentration in the major part of zone B is higher, and there is a small portion of

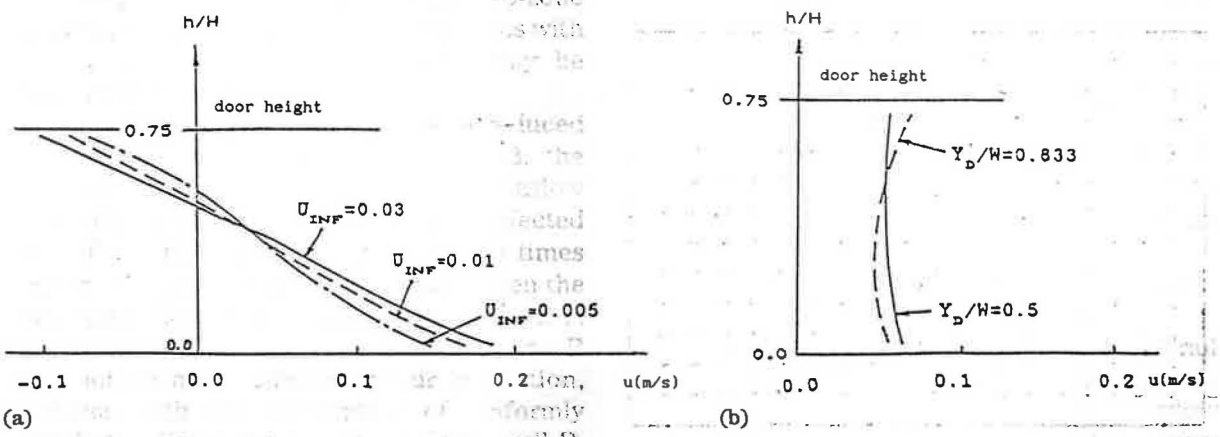

Fig. 5. (a) Distributions of velocity component in the x direction at door opening for the case with $y_D/W=0.167$. (b) Distributions of velocity component in the x direction at door opening for the cases with $y_D/W=0.5$ and 0.833 ($U_I=0.03$ m/s).

TABLE 3. Average concentration in each zone

Infiltration	−0.005 m/s	−0.01 m/s	−0.03 m/s
Zone A	3.941	2.820	0.874
Zone B	6.033	4.390	2.158

contaminant which migrated into zone A from zone B.

The distributions of the velocity component in the x direction at the axis of the door opening under infiltration velocity 0.03 m/s are presented in Fig. 5(b). With a centrally located door opening, the velocity component in x direction, u, is more uniform than that for the case when the door opening is close to the northern wall and to the exhaust opening. The suction at the exhaust may cause a low pressure, which works as a sink term for the momentum equation in the x direction. Comparing Fig. 5(b) with 5(a), for the same infiltration flow rate, there is a counter-airflow from zone B to zone A only when the door opening is at $y_D/W = 0.167$. It may be explained as follows. The exhaust is closer to the door opening when y_D/W is equal to 0.5 or 0.833, therefore, the influence of the suction at exhaust opening would be stronger in these cases. It enhances the air movement from zone A to zone B. Thus, it could be understood that if zone A is expected to be free from the contaminant generated in zone B, the overall arrangement may be more crucial than the magnitude of the infiltration rate.

6. Conclusions

The isothermal airflow and contaminant distribution in a two-zone enclosure with forced convections are studied by numerical technique. The infiltration effects on the ventilation airflow are examined by varying the infiltration flow rate from 1.8 ach to 10.8 ach while the

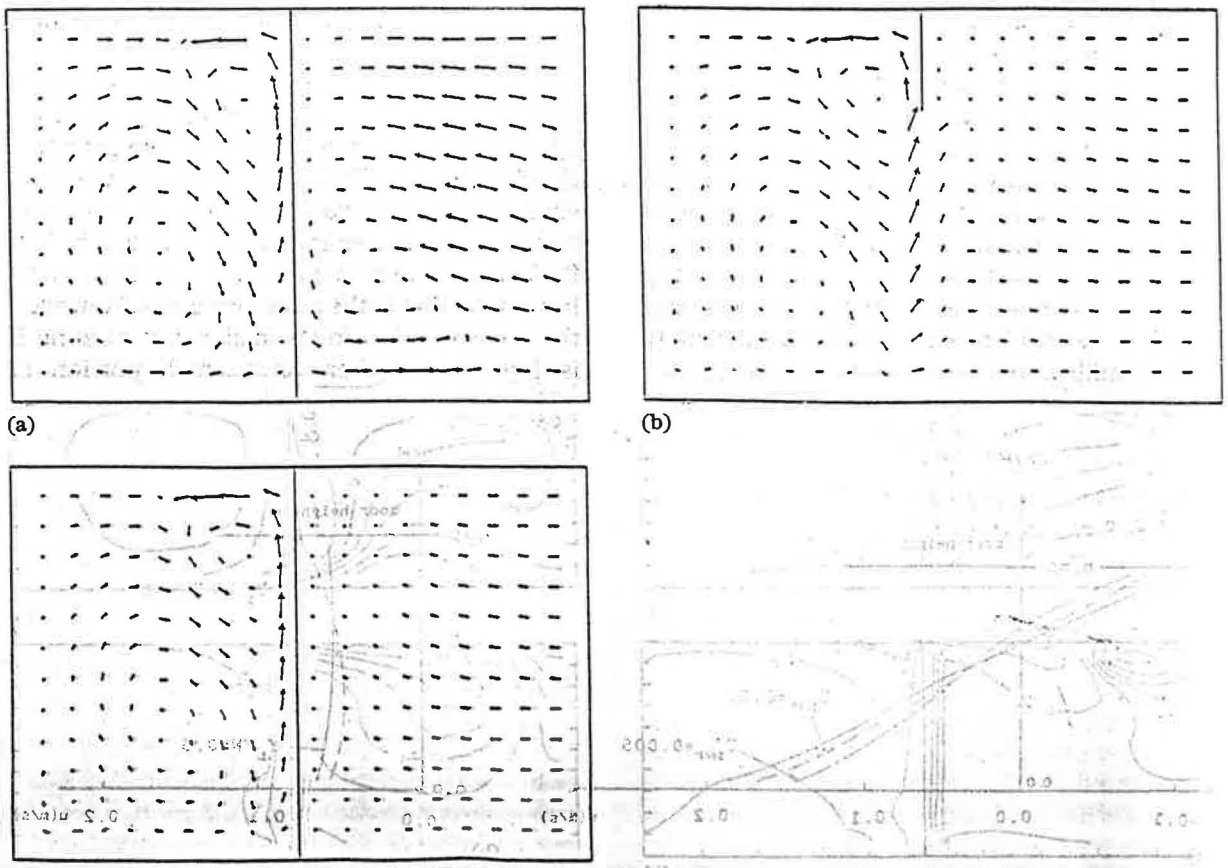

Fig. 6. Velocity vectors in vertical section $y/W = 0.46$. (a) $y_D/W = 0.167$, maximum vector 0.782E−1. (b) $y_D/W = 0.50$, maximum vector 0.114. (c) $y_D/W = 0.833$, maximum vector 0.115.

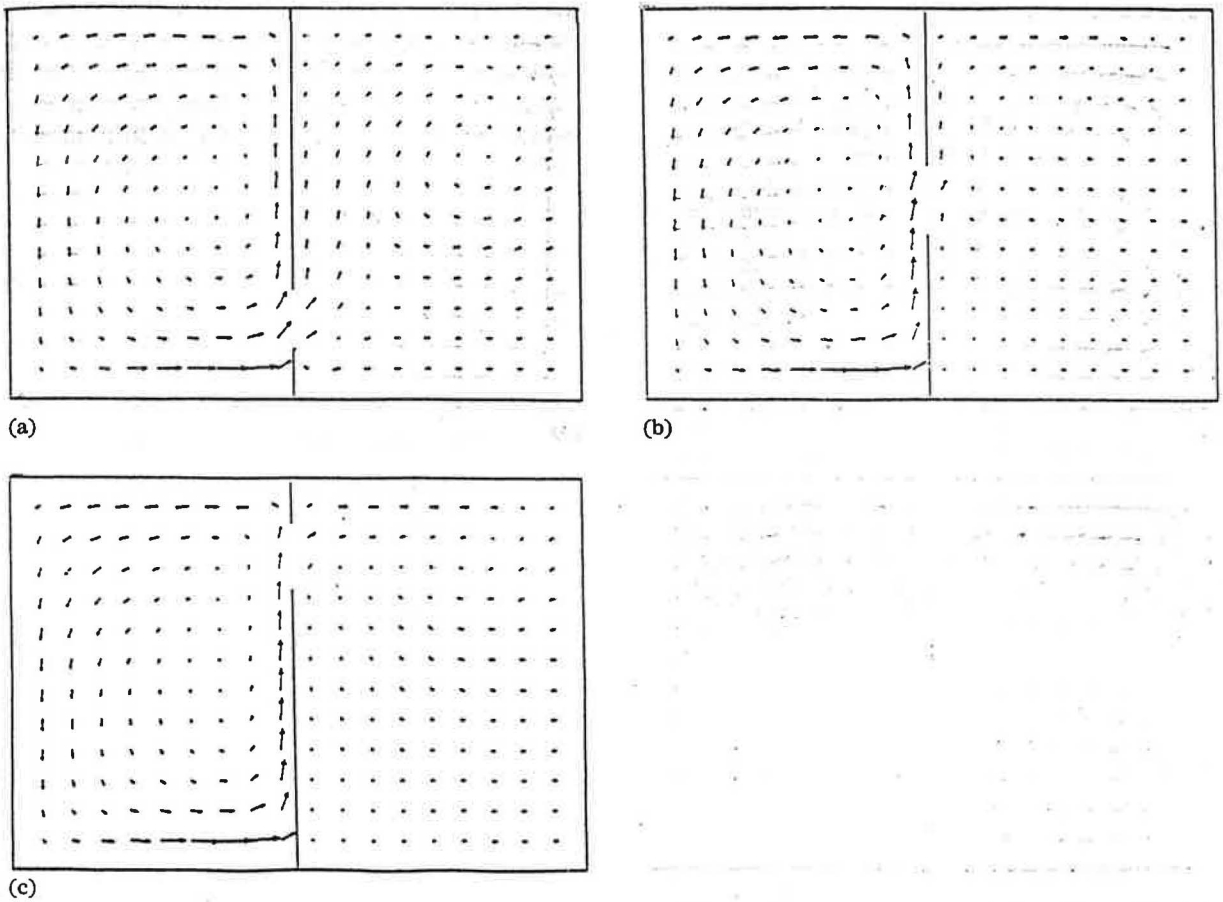

Fig. 7. Velocity vectors in horizontal section $z/H=0.29$. (a) $y_D/W=0.167$, maximum vector 0.264. (b) $y_D/W=0.5$, maximum vector 0.270. (c) $y_D/W=0.833$, maximum vector 0.276.

ventilation flow rate and door position are fixed. The effects of door position on the flow pattern and contaminant dispersion are investigated by placing the door opening at $y_D/W=0.167$, 0.5 and 0.833 respectively. For the two-zone enclosure under this study, and enclosures with the similar layout, the conclusions may be summarized as follows:

(1) When the ventilation air is introduced into zone A and released from zone B, the infiltration flow could only affect the airflow in zone B. Zone A does not seem to be affected even if the infiltration flow rate is three times higher than the ventilation flow rate. When the infiltration flow rate is about the same level as ventilation flow rate, the airflow in zone B may not be much affected by air infiltration, because, with the assumption of uniformly distributed air infiltration on the entire wall E, the momentum of infiltration flow is much smaller than that of ventilation.

(2) When there is a local exhaust above the contaminant source and the door opening is placed properly, the contaminant in the infiltration zone could hardly migrate into the ventilation zone, even if the infiltration flow rate is relatively high.

(3) The flow pattern in zone A is not sensitive to the door opening position. This is due to the effect of the local exhaust system in zone B, which weakens the infiltration airflow before it reaches the door opening. Thus, the flow pattern in zone A is mainly independent of the infiltration flow.

(4) The flow pattern in zone B is significantly affected by the door opening position.

In the attempt to make a reasonable overall arrangement with openings of supply, exhaust and door, the detailed information about airflow pattern and contaminant distribution is always required. For a fixed arrangement of openings, the airflow could be different due to buoyancy

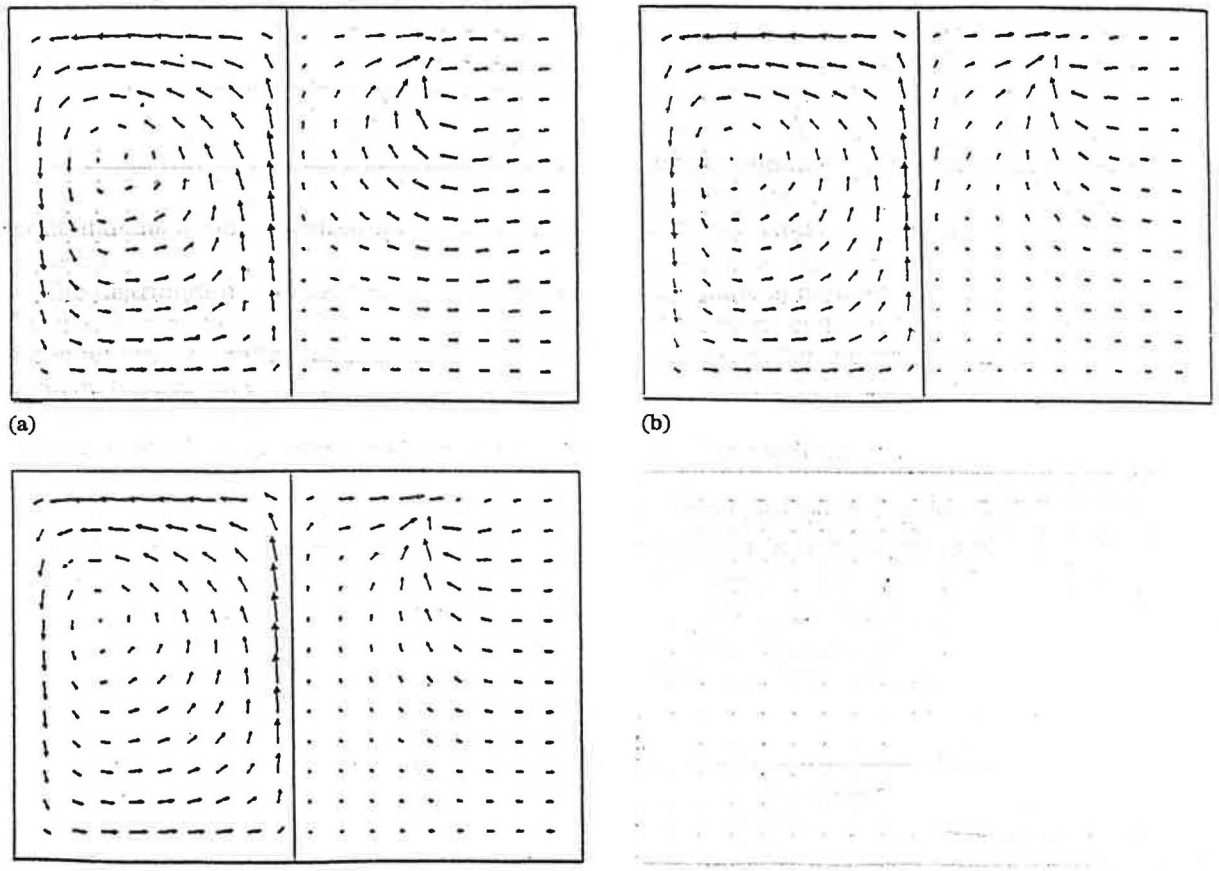

Fig. 8. Velocity vectors in horizontal section $z/H=0.79$. (a) $y_D/W=0.167$, maximum vector 0.126. (b) $y_D/W=0.5$, maximum vector 0.159. (c) $y_D/W=0.833$, maximum vector 0.162.

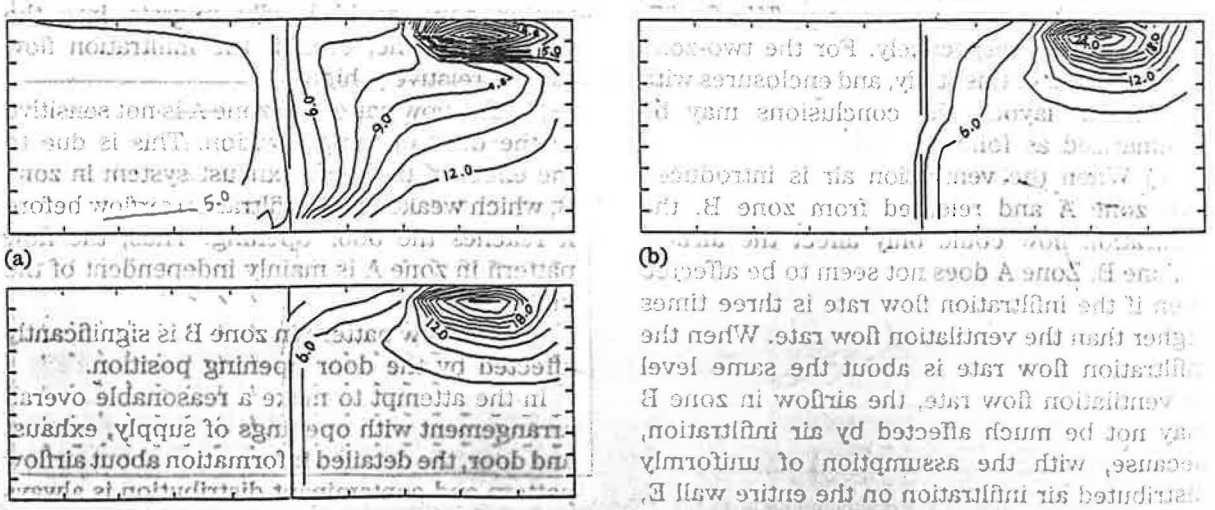

Fig. 9. Contaminant contours in horizontal section $z/H=0.29$. (a) $y_D/W=0.167$. (b) $y_D/W=0.50$. (c) $y_D/W=0.833$.

and/or air infiltration. The numerical simulation is a useful tool to predict these phenomena in various flow situations. The results presented here give a clear picture and qualitative understanding of the infiltration influence on the isothermal airflow in a ventilated, partitioned enclosure.

List of symbols

A_i	area of control volume interface perpendicular to the x-direction
b	opening width
c	contaminant concentration
C_μ	0.09, a constant in the turbulent model
C_1, C_2	constants in the turbulent model
G_k	the generation rate of turbulent energy
H	room height
h	opening height
k	kinetic energy of turbulence
L	room length
l	the dimension of exhaust opening in x direction
p	pressure
Q	volume flow rate
Q_{up}	upstream volume flow rate
Re	Reynolds number, $U_I h_I/\nu$
S_ϕ	source term for ϕ
t	time
u, v, w	velocity components in x, y, z direction respectively
U_I	air velocity at ventilation inlet
U_{INF}	air infiltration velocity
x, y, z	Cartesian coordinate system
W	width of room

Greek symbols

Γ	exchange coefficient
ϵ	dissipation rate of k
μ	dynamic viscosity
ν	kinematic viscosity
ρ	density
σ	Prandtl or Schmidt number
ϕ	variable

Subscripts

D	door
eff	effective
E	exhaust opening
I	supply inlet
t	turbulent

References

1 G. N. Walton, Airflow network models for element-based building airflow modeling, *ASHRAE Trans., 95* (2) (1989) 611–620.

2 Q. Y. Chen, J. Van der Kooi and A. Meyers, Measurements and computations of ventilation efficiency and temperature efficiency in a ventilated room, *Energy Build., 12* (1988) 85–99.

3 F. Haghighat, P. Fazio and J. Rao, A procedure for measurement of ventilation effectiveness in residential buildings, *Build. Environ., 25* (2) (1990) 163–172.

4 P. V. Nielson, Contaminant distribution in industrial area with forced ventilation and two-dimensional flow, *Proc. IIR-Joint Meeting, Commission E1, Essen, F.R.G., 1981*, Vol. 5, pp. 223–230.

5 S. Kato, S. Murakami and S. Chirfu, Study on air flow in conventional flow type clean room by means of numerical simulation and model test, Inst. of Industrial Sci., Univ. of Tokyo, Japan, *Ann. Rep. of Group Research Activity on Numerical Simulation of Turbulent Flow, Number 2*, 1986, also *Proc. 8th Int. Symposium on Contaminant Control, Milan, 1986*, pp. 781–791.

6 P. Berne and M. Villard, Prediction of air movement in a ventilated enclosure with 3-D thermohydraulic code TRIO, *Proc. Conf. ROOMVENT-87, Stockholm, 1987*, Vol. 3, pp. 1–15.

7 R. H. Horstman, Predicting velocity and contamination distribution in ventilated volumes using Navier-Stokes equations, *Proc. ASHRAE Conf., IAQ 88, Atlanta, GA, April 11–13, 1988*, pp. 209–230.

8 L. C. Chang, J. R. Lloyd and K. T. Yang, A finite difference study of natural convection in complex enclosures, *Proc. 7th Int. Heat Transfer Conf., 1982, München*, Vol. 2, pp. 183–188.

9 K. M. Kelkar and S. V. Patankar, Numerical prediction of natural convection in partitioned enclosures, *Numerical Heat Transfer, 8* (1985) 63–71.

10 F. Haghighat, Z. Jiang and J. C. Y. Wang, Natural convection and air flow pattern in a partitioned room with turbulent flow, *ASHRAE Trans., 95* (2) (1989) 600–610.

11 M. W. Nansteel and R. Greif, An investigation of natural convection in enclosures with two and three dimensional partitions, *Int. J. Heat Mass Transfer, 27* (4) (1984) 561–571.

12 D. Scott, R. Anderson and R. Figliola, Blockage of natural convection boundary layer flow in a multizone enclosure, *Int. J. Heat Fluid Flow, 9* (2) (1988) 208–214.

13 M. Epstein, Buoyancy-driven exchange flow through small openings in horizontal partitions, *J. Heat Transfer, Trans. ASME, 110* (1988) 885–893.

14 J. Neymark, A. Kirkpatrick, R. Anderson and C. Boardman, High Rayleigh number natural convection in partially divided air and water filled enclosures, *Proc. National Heat Transfer Conf., Houston, 1988*, pp. 1–8.

15 C. R. Boardman, A. Kirkpatrick and R. Anderson, Influence of aperture height and width on interzonal natural convection in a full-size, air-filled enclosure, *ASME HTD, Vol. 107*, 1989, Heat Transfer in Convective Flows, pp. 273–280.

16 F. Haghighat, J. C. Y. Wang and Z. Jiang, Three-dimensional analysis of airflow pattern and contaminant dispersion in a ventilated two-zone enclosure, *ASHRAE Trans.*, *96* (1) (1990) 831–839.
17 A. D. Gosman, P. V. Nielsen, A. Resting and J. H. Whitelaw, The flow properties of rooms with small ventilation openings, *J. Fluids Eng., Trans. ASME*, *102* (1980) 316–323.
18 W. Rodi, *Turbulence Models and their Application in Hydraulics — A State-of-the-Art Review*, Karlsruhe, F.R.G., 2nd revised edn., 1984.
19 S. V. Patankar, *Numerical Heat Transfer and Fluid Flow*, Hemisphere, 1980.
20 B. E. Launder and D. B. Spalding, The numerical computation of turbulent flows, *Comput. Meth. Appl. Mech. Eng.*, *3* (1974) 269–289.